ISSN 1070-3632, *Russian Journal of General Chemistry, 2008, Vol. 78, No. 11, pp. 2247–2256. © Pleiades Publishing, Ltd., 2008.*
Original Russian Text © R. Meallet-Renault, G. Clavier, C. Dumas-Verdes, S. Badre, E. Yu. Shmidt, A.I. Mikhaleva, C. Laprent, R. Pansu, P. Audebert, B.A. Trofimov, 2008, published in Rossiiskii Khimicheskii Zhurnal, 2008, Vol. 52, No. 1, pp. 91–99.

Novel BODIPY Preparations from Sterically Hindered Pyrroles. Synthesis and Photophysical Behavior in Solution, Polystyrene Nanoparticles, and Solid Phase

R. Meallet-Renault[a], G. Clavier[a], C. Dumas-Verdes[a], S. Badre[a], E. Yu. Shmidt[b], A. I. Mikhaleva[b], C. Laprent[a], R. Pansu[a], P. Audebert[a], and B. A. Trofimov[b]

[a] *PPSM, ENS Cachan, CNRS, UniverSud, 61 av. President Wilson, F-94230 CACHAN, France*
[b] *Favorskii Irkutsk Institute of Chemistry, Siberian Branch, Russian Academy of Sciences,*
ul. Favorskogo 1, Irkutsk, 664033 Russia
e-mail: boris_trofimov@irioch.irk.ru

Received February 15, 2008

Abstract—Trimesityl-BODIPY (TMB), a new derivative of 4,4-difluoro-4-bora-3a,4a-diaza-*s*-indacene belonging to fluores-cent nanostructures series, was synthesized from the corresponding pyrrole by the Trofimov reaction. This reaction was also employed to obtain 2-[2.2]paracyclophanylpyrrole from 5-acetyl[2.2]-paracyclophane. The spectral properties of TMB have been investigated in dichloromethane, nanolatex (polystyrene) films prepared by rapid solvent evaporation, and microcrystals. Comparative analysis of TMB properties with those of mesityl-BODIPY (MB) was performed. TMB was prepared to minimize π–π interactions in order to preserve luminescence in the aggregate state. Both fluorophores were shown to form fluorescing aggregates in the amorphous state (film). Fluorescence spectra (extinction and lifetime) were also studied. In crystal, MB shows a weaker fluorescence, while TMB behaves as a single fluorescing aggregate with a lifetime of 9.5 ns.

DOI: 10.1134/S1070363208110467

INTRODUCTION

Fluorescence spectroscopy is used for structural and dynamic studies on both organic and inorganic systems. The success of this technique is due to a great sensitivity of fluorophores to their immediate environment [1]. Fluorescence can be used for high-precision physicochemical and biochemical measurements. The technical possibilities of fluorescence spectroscopy allow spectra of a single molecule to be measured [2]. The fluorescence technique has found application in biochemical [3], medical chemical [4], and environmental analysis [5].

The popularity of fluorescence spectroscopy favored extension of the range of organic and inorganic fluorophores. They can be used in a variety of ways, mostly as labels [6]. However, certain limitations can arise because of fluorescence quenching and decreased quantum yields. Alternative approaches were developed, such as use of dendrimers [7] which still remain fairly expensive materials, fluorescent polymers [8], zeolites [9] or activated latex spheres, as well as inorganic nanocrystals (quantum points) [10]. Organic crystals or pigments [11] are, in principle, quite attractive candidates, since they allow one to create a high local fluorophore concentration and ultrabright objects [12], but, unfortunately, very little fluorophores are able to form radiating crystals. Actually, aggregation suppresses fluorescence [13] due to interactions between molecular electron clouds, which increases the probability of radiationless transitions [14].

Over some years we have synthesized various fluorescing crystals, aimed at obtaining novel radiating derivatives of 4,4-difluoro-4-bora-3*a*,4*a*-diaza-*s*-indacene which is better known under the registered trade mark BODIPY®.

These chromophores and, especially, their polysubstituted derivatives possess optimal spectral characteristics (high fluorescence quantum yield, high radiative stability) [15], and, at the same time, are

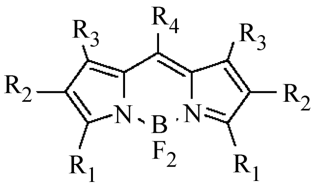

BODIPY

readily synthesized from pyrrole derivatives [16]. Our approach is based on the use of BODIPY nanocrystals or dispersions in latex nanospheres and aimed at producing ultrasensitive fluorescent sensors.

It was shown that fluorescence quenching in the solid phase can be limited or avoided if fluorophores are locates at a certain distance from each other [17]. With this in mind we synthesized sterically hindered pyrroles and then used them as starting materials for preparing BODIPY derivatives capable of forming fluorescing crystals. These compounds can also be introduced in polymer nanoparticles [18] without the risk of fluorescence quenching on aggregation. Moreover, substitution in the pyrrole ring shifts the absorption spectrum of the resulting derivatives to lower energies [19].

Here we report on the synthesis of pyrroles with sterically hindered substituents by the Trofimov reaction and their subsequent transformation into BODIPY. Detailed information on the photophysical properties of the products in solution and in the solid phase is also presented.

Synthesis of BODIPY

Synthesis of BODIPY was performed in three stages: condensation of aldehyde with two pyrrole molecules, oxidation, and complex formation with boron trifluoride (Scheme 1). Intermediate products were not isolated.

Burgess and co-workers [20] suggested a new approach, by replacing aldehyde with acid chloride (Scheme 2).

The molecular geometries were calculated quantum-chemically for structures with the lowest gas-phase energy.

This procedure does not involve isolation of the intermediate indacene and oxidation with DDQ (dichlorodicyanobenzoquinone), which offers great advantages by excluding by-product formation. The procedure involves prolonged heating (24 h with stirring in a solvent), but the reaction yield is generally higher.

The first BODIPY derivative (MB) was prepared by condensation of cryptopyrrole with mesitylaldehyde (Scheme 3) in 70% yield [21].

Solid-phase photophysical properties of the resulting derivative proved to be quite reasonable (vide

Scheme 1. *Synthesis of BODIPY by condensation of pyrrole with aldehyde.*

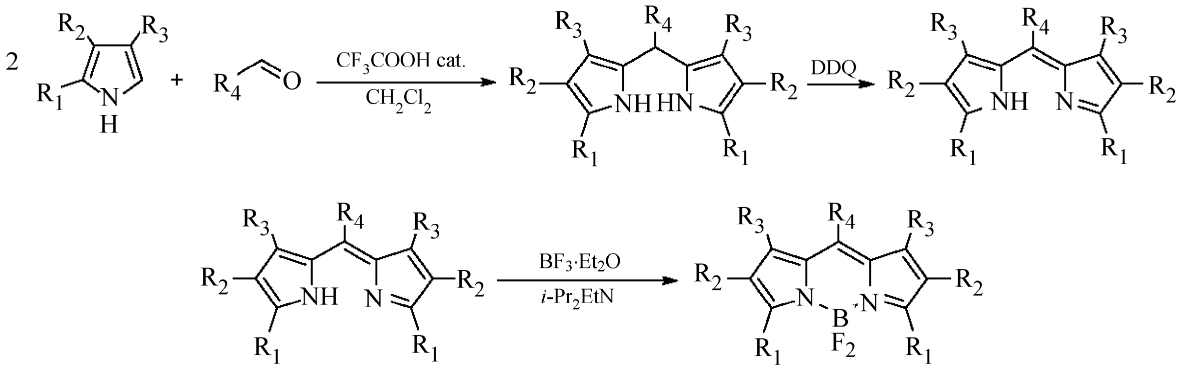

Scheme 2. *Synthesis of BODIPY by Burgess by condensation of pyrrole with acid chloride.*

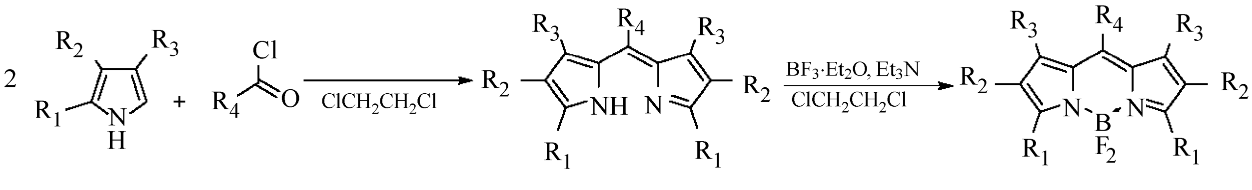

Scheme 3. Synthesis of MB.

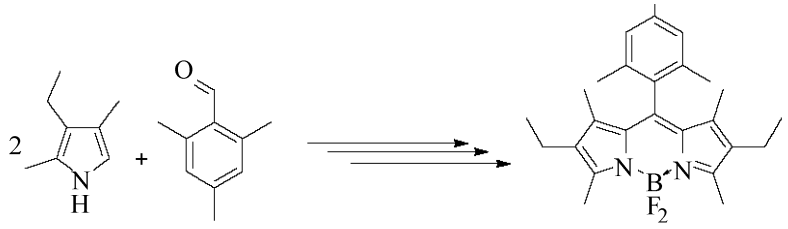

supra). In the meantime, pyrroles with bulkier substituents were prepared by the Trofimov reaction, involving condensation of oximes with acetylenes in a superbasic medium (Scheme 4) [22].

Scheme 4. Trofimov reaction.

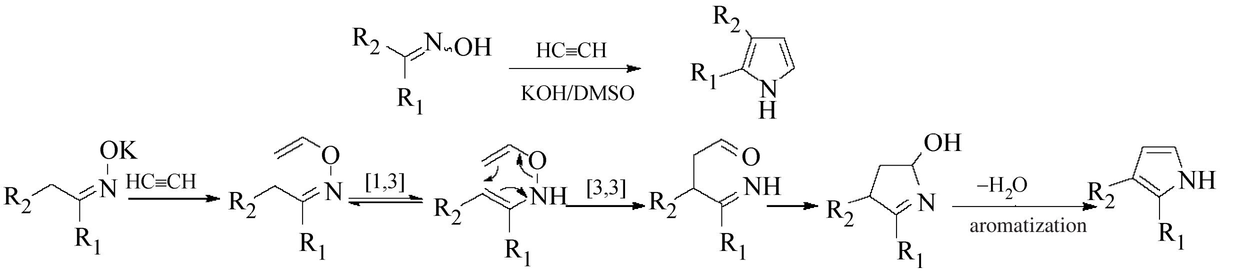

This reaction allows an almost infinite range of pyrroles to be synthesized from acyl oximes and acetylene.

In the present we took two aromatic compounds: mesitylene and [2.2]paracyclophane. Difficulties arose in the synthesis of ethyl mesityl ketone oxime. It was found that ethyl mesityl ketone (I) is quite poorly reactive toward hydroxylamine. Oximation by refluxing the ketone with hydroxylamine hydrochloride under varied conditions, including microwave activation, proved ineffective. “Lethargic oximation” (over the course of 8 months) gave as little as 30% of ethyl mesityl ketone oxime (II) (Scheme 5).

Scheme 5. “Lethargic” synthesis of ethyl mesityl ketone oxime.

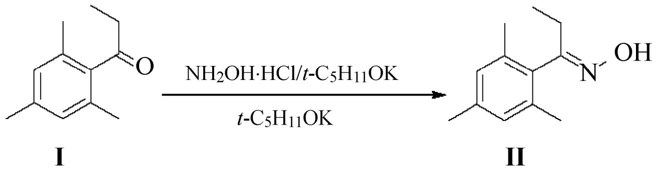

A different synthetic approach to oxime II was also used: Mesitylmagnesium bromide (IV) was reacted with propionitrile to form the corresponding imine whose oximation gave the target oxime (total yield ~40%). The whole procedure can be accomplished within two days.

Scheme 6. Alternative synthesis of ethyl mesityl ketone oxime.

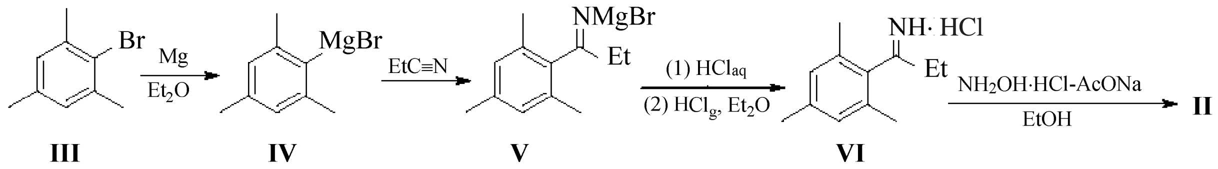

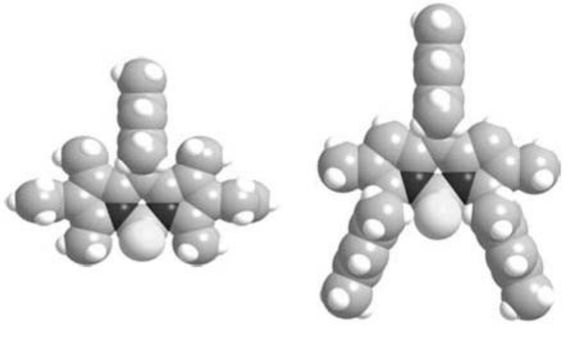

Fig. 1. Gas-phase structures of MB and TMB, obtained by B3LYP/6-31G*(d) minimization.

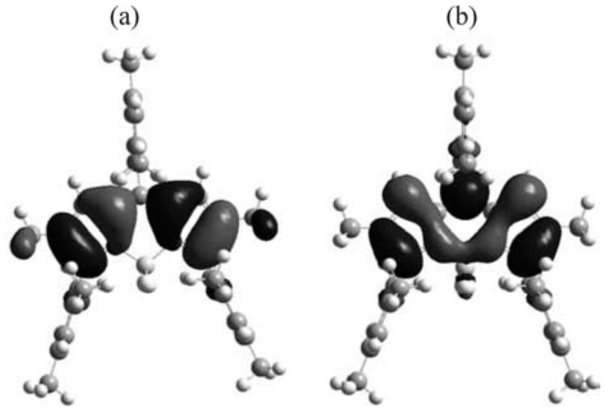

Fig. 2. (a) OH and (b) и BV molecular orbitals of TMB.

In 5-acetyl[2.2]paracyclophane, steric hindrances are expressed to a lesser extent. In this case, oxime can be easily prepared in high yield (97%) by direct oximation of ketone with hydroxylamine.

Pyrroles were synthesized by reacting oximes with acetylene in the presence of the KOH/DMSO superbase. With ethyl mrsityl ketone oxime, the corresponding pyrrole was obtained in 23% yield at an atmospheric pressure of acetylene. Under the same conditions, the yield of pyrrole from 5-acetyl[2.2]-paracyclophane oxime was as little as 10–15%. This result can be explained by deoximation of the target oxime under the reaction conditions. An alternative approach was suggested, that involved initial formation of anhydrous cesium oximate and subsequent reaction in the presence of acetylene at *p* 14 atm to obtain pyrrole in a total yield of 41% [23].

Similarly, BODIPY TMB was synthesized by condensation of 2-mesityl-3-methylpyrrole in 45% yield.

Molecular Modeling

The two obtained BODIPY derivatives were modeled (Fig. 1) by the DFT method [24].

The central indacene in both molecules is planar, and the mesityl rings embraced between the 2- and 6-Me groups are inclined to the indacene plane by 90°. Thus, the aromatic systems serve as good bulky substituents that do not violate the fine structure of the central fragment in BODIPY. These results are consistent with data Kee et al. [25], who showed that the steric hihindrances associated with the substituent R_4 in the BODIPY molecule much affect the fluorescence properties of BODIPY.

Comparison of the two structures shows that the three bulky substituents in the TMB molecule should hinder intermolecular interactions. It can be expected that TMB should surpass MB in solid-phase photophysical properties. The $S_0 \rightarrow S_1$ transition in BODIPY occurs between the HO and BV orbitals (see Fig. 2) [26].

In TMB, these two orbitals are localized on the central indacene and have nothing in common with the aromatic rings at the molecular periphery. The same result is observed with MB. Substituents have no effect on the positions of the absorption and emission bands of MB and TMB derivatives.

Spectrometric Studies
Fluorescence in Solution

The absorption and fluorescence spectra of MB and TMB are shown in Fig. 3.

The absorption maxima are at 526 and 543 nm and correspond to the $S_0 \rightarrow S_1$ transition There is also one more absorption band near 350 nm, assignable to the $S_0 \rightarrow S_2$ transition. the emission maxima ($S_1 \rightarrow S_0$) are at 535 and 556 nm for MB and TMB, respectively. The red shift of the maximum is due to the inductive effect of mesityl groups. Such spectral pattern is characteristic of all molecules of the BODIPY family. The molecular extinction coefficients of MB and TMB and the fluorescence quantum yields are fairly high (Table 1).

The excitation spectra coincide with the absorption spectra. The fluorescence lifetime in dichloromethane is ~6 ns (±0.1). Both fluorophores are stable under light irradiation (no changes were observed under light irradiation at 200 mW cm^{-2}).

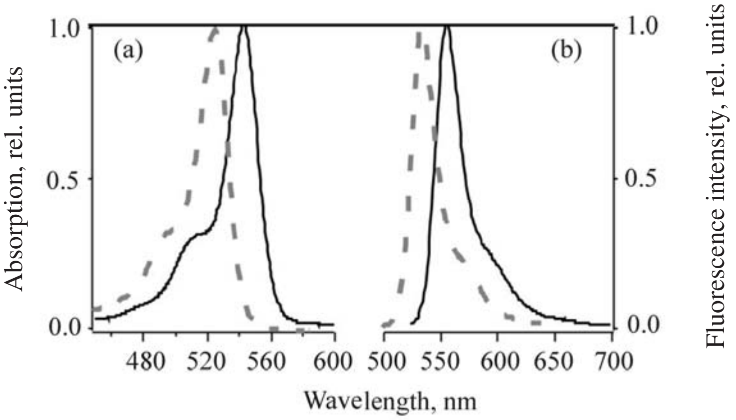

Fig. 3. (a) Absorption and (b) emission spectra in dichloromethane: (dashed line) MB and (solid line) TMB.

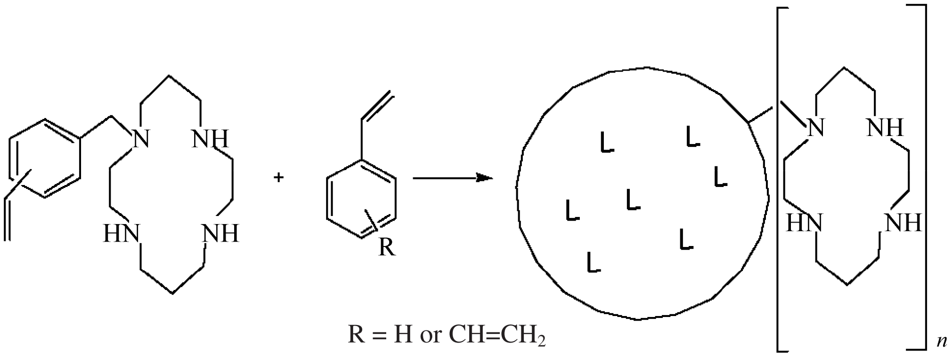

R = H or $CH=CH_2$

Fig. 4. Scheme of synthesis of polystyrene nanoparticles with cyclam groups.

Earlier a BODIPY containing a 4'-iodophenyl substituent in the 4 position of the pyrrole ring was synthesized. The properties of this BODIPY in chloroform are quite similar to those of MB. Burghart and co-workers [27] synthesized an analog of TMB containing a 4'-iodophenyl substituent in the 4 position and a phenyl substituent in the 1 position. However, this latter BODIPY has a much lower fluorescence quantum yield (0.2 in $CHCl_3$), since phenyl rotation gives rise to radiationless transitions. Blocking such rotation much enhances the quantum yield [25, 27]. Rotation of mesityl groups about the C–aryl bond in TMB is hindered. This fact explains the observed high fluorescence quantum yield.

Activated Polystyrene Nanoparticles

We embedded MB molecules in polymer balls (Fig. 4).

These particles contain both surface and central cyclam groups (L) that can associate with Zn(II), Cu(II), and Ni(II) ions (Table 2).

Latex 15 nm in diameter is stable in aqueous suspension in the presence of a surfactant (dodecyltrimethylammonium bromide, 15–0.05 wt %).

Balls have different colors depending on the nature of the metal ion in the solution (Fig. 5). They are colorless in straight water and get bluish violet, if Cu (II) ions are added. Balls were impregnated with MB molecules by swelling in dichloromethane. Organic

Table 1. Characteristics of the absorption and fluorescence spectra in dichloromethane[a]

BODIPY derivative	Absorption maximum, λ_{ads}, nm	Fluorescence maximum, λ_{em}, nm	Extinction coefficient, ε, $l\,mol^{-1}\,cm^{-1}$	Lifetime, τ, ns	Quantum yield, Φ_f
MB	526	535	58000	6.10	0.72
TMB	543	556	80000	6.30	0.90

[a] χ^2 (MB) 1.058; χ^2 (TMB) 0.969.

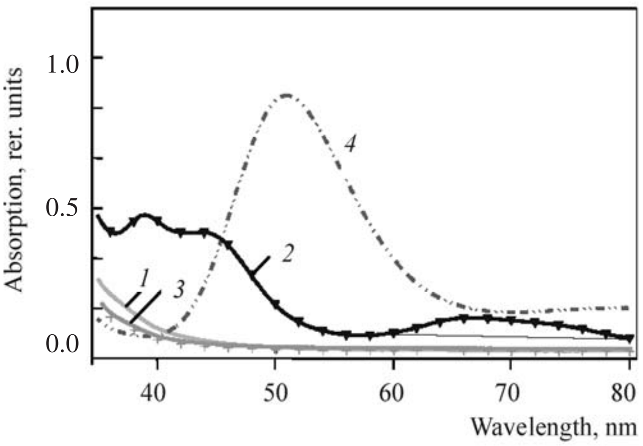

Fig. 5. Absorption spectra of cyclams: (*1*) free cyclam ligands; (*2*) cyclam–nickel complex; (*3*) cyclam–zinc complex; and (*4*) cyclam–copper complex.

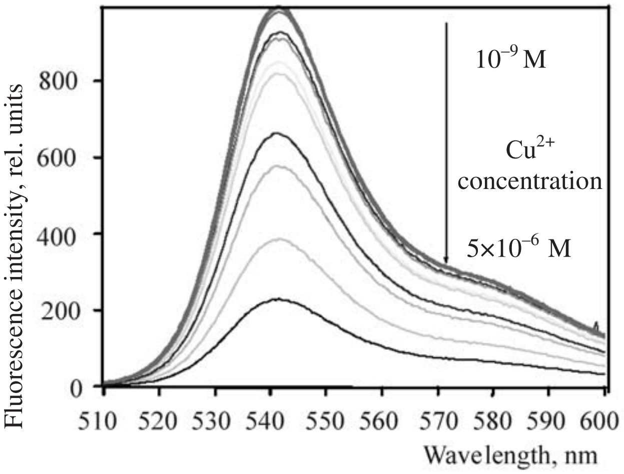

Fig. 6. Fluorescence spectrum of nanolatex containing MB molecules in the presence of Cu^{2+}.

solvent discloses nanoparticles, the hydrophobic fluorophore escapes the aqueous medium and penetrates into balls that contract when the solvent is evaporated. Therewith, the spectral properties of MB change only slightly (λ_{ads} 528.5 nm, λ_{em} 540 nm, fluorescence quantum yield 0.77). It was shown that one ball can accommodate 70–80 MB molecules without changing its size and color. When more MB molecules are inserted (up to 110 molecules per ball), the system gets less stable (it loses color within several months). Red shifts of the absorption and emission spectra and decreased fluorescence lifetimes and quantum yields were also noted, imply-ing formation of nonradiating aggregates.

The samples containing 75 fluorophore molecules per ball are selective toward Cu(II). Actually, it is only these ions that are able to quench fluorescence (Fig. 6); thus, the detection limit of copper ions is about 1 nmol l^{-1} (0.03 copper ions per ball).

Nickel and zinc ions have no effect on fluorescence. Such selectivity can be explained in terms of energy transfer from fluorophore to colored complex, since the spectrum of the cyclam–copper complex much overlaps with the emission spectrum of MB.

Analysis of spectral data shows that inside particles fluorophore can be present in two different states. The fluorescence of 80% chromophore molecules is quenched by the cyclam–copper complex, and the rest 20% preserve their initial properties. This finding allows us to state that 20% fluorophore molecules reside in the very center of the particles. On the other hand, fluorescence quenching is quite efficient (9% quenching at the ion concentration 5 nmol l^{-1}), which can be explained by the antenna effect (energy jump on Forester's transfer) between BODIPY molecules enclosed in the particle. Evidence for this conclusion comes from fluorescence anisotropy measurements.

By embedding BODIPY family particles in nanoparticles, we could enhance the sensitivity of a colorimetric sensor toward Cu^{2+} ions.

We also embedded TMB molecules in nanoparticles whose surface was modifies with cyclam groups [28]. These nanoparticles have almost the same spectral properties as free TMB molecules (λ_{ads} 545 nm, λ_{em} 559 nm, τ_F 7 ns), but no more than 40 molecules can be embedded in one ball, and, therewith, reduced solubility of the dye outside the matrix is observed. The molecular size of TMB (ca. 15×10×5 Å) is larger compared to MB (ca. 10×10×5 Å), and the polymer has a different structure if the cyclam

Table 2. Association constants of cyclam with metal ions

Parameter	Cu(II)	Ni(II)	Zn(II)	Co(II)	Cd(II)
Association constant	10^{27}	10^{20}	10^{20}	10^{13}	10^{11}
Ball color in solution	Bluish violet	Bluish green	Colorless	–	Colorless

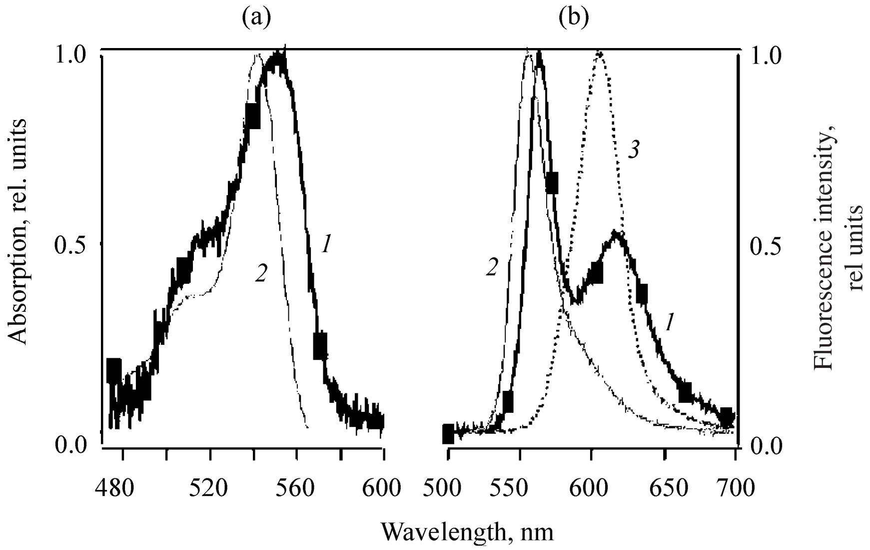

Fig. 7. (a) Absorption and (b) emission spectra of TMB: (*1*) in film; (*2*) in dichloromethane; and (*3*) in monocrystal.

ligand is grafter exclusively to the surface and is not contained inside balls. By this reason, one nanolatex particle binds more MB than TMB molecules. Experiments on TMB fluorescence quenching with metal ions are in progress.

As mentioned above, aggregation of balls with high MB contents took place, which followed from changes in certain fluorescence parameters. The properties of MB and TMB in amorphous films and crystal powders were also studied.

Amorphous Films

Amorphous MB and TMB films can be obtained by rapid solvent evaporation. Inspection of the fluorescence spectra reveals micrometer-sized drops at a distance of a few nanometers from each other.

Figure 7 shows the absorption and emission spectra of a TMB film.

Compared with the dichloromethane solution, the absorption spectrum is broader, and its maximum is shifted red ($\Delta\lambda$ 10 nm). The fluorescence spectra contain two maxima: 569 ± 4 and 619 ± 2.9 nm (Table 3).

Multiexponential fluorescence decay is observed, and the apparent lifetime is shorter than for monomeric molecules in solution (from 0.5 to 1.5 ns).

According to Kasha's aggregation model [28], the molecular dipoles in J-type aggregates are oppositely directed (Fig. 8): An allowed transition from the ground state to a lower energy level takes place.

In the lower part of the figure we present a scheme of dipole orientation in the ground and higher excited fluorophore states. The absorption spectrum is shifted red, relaxation is faster, and lifetime is shorter than for the monomer in solution. The first absorption range is contributed by monomeric TMB molecules, and the second is definitely associated with J-type aggregates.

Our aim was to decrease the "monomer contribution" (λ_{em} ~ 569 nm) into image formation over the fluorescence lifetime of the aggregates ($\lambda_{em.}$~ 619 nm) (Fig. 9). To this end, we made use of filters to "isolate" accessible wavelength ranges.

Table 3. Spectral data for amorphous films and crystal powders

Object	λ_{ads} , nm	λ_{em}, nm	<τ> , ns
MB film	542	562 635 739 (peak)	1. 36
MB powder		608 739	1. 28
TMB film	553	569 619	0. 5–1. 5
TMB powder	–	598	1. 77
TMB microcrystal	–	608	9.5[a] [1.087][b]

[a] Monoexponential decay. [b] χ^2.

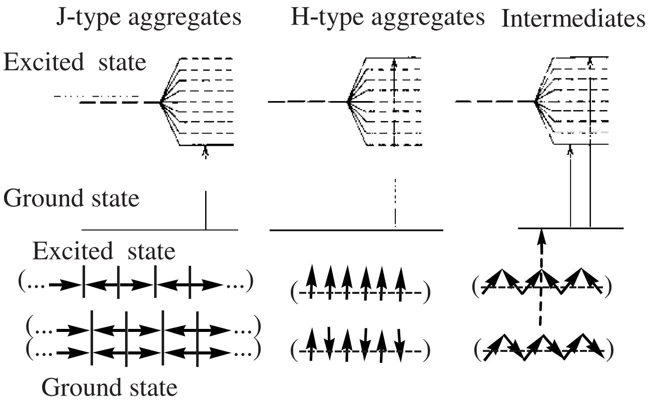

Fig. 8. Diagram of exciton states and schematic representation of dipole orientation in aggregates in different states [29].

The “monomer contribution” (560-nm filter) can be observed in Fig. 9b: a homogeneous image over the entire sample, both in terms of intensity and in terms of lifetime. It should be noted that the lifetime for the monomer is much smaller than in the case of the total fluorescence yield (entire wavelength range, Fig. 9a). Probably, the monomer monotonically decreases emission: fluorescence quenching occurs.

The “aggregate contribution” (619-nm filter) into the intensity of the image is nonuniform over the sample (Fig. 9c), implying that the aggregate is inhomogeneous; the lifetime is longer than for the monomer.

Together the above evidence suggests that the principal form here is the monomer. Intensity visualization shows that it is distributed homogeneously, and its emission is quenched due to aggregate formation.

The absorption spectrum of MB films is broader compared to the monomer and shifted red (Table 3). The fluorescence spectra contain a broad band with at 562±3.5 nm (in some cases, additional broadening at 635 nm is observed) and a band at 739.5±1 nm. The mean lifetime is 1.36±0.07 ns. Thus, we can suggest that J-type aggregates are also formed in amorphous films.

Microcrystals

We obtained fluorescence spectra for MB and TMB crystal powders. Compared with the above-described amorphous films, the fluorescence spectra of TMB crystal powders are much broader and contain a single

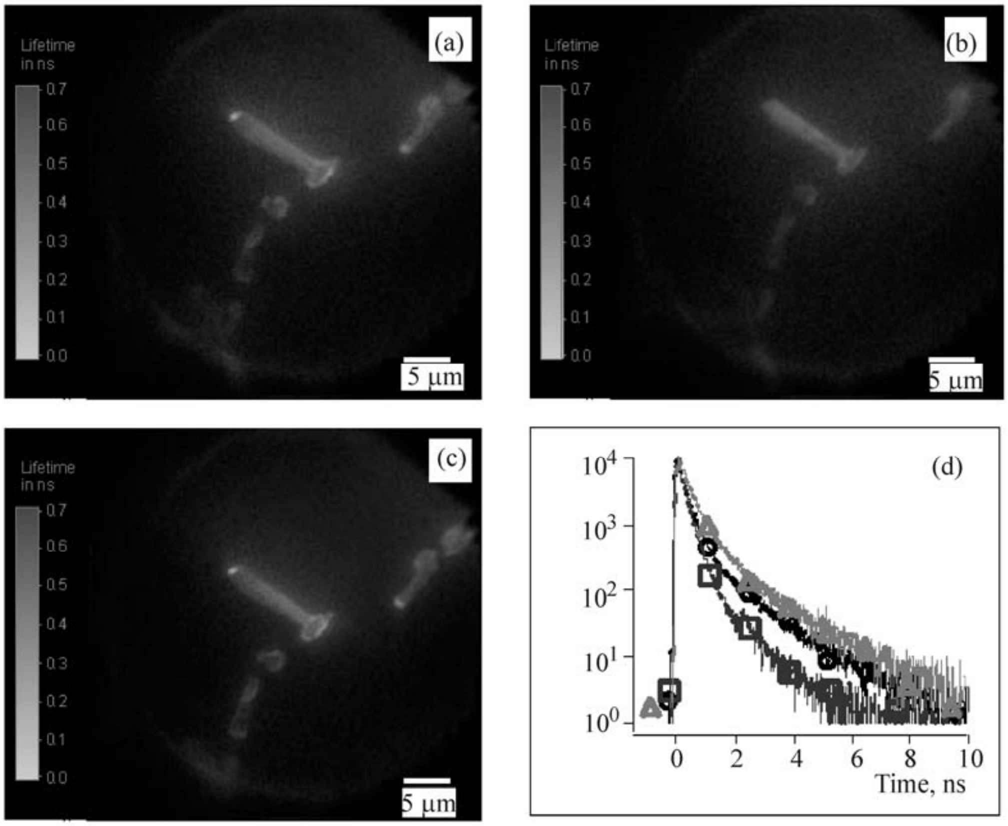

Fig. 9. Images of amorphous films of TMB: (a) full spectrum; (b) monomer contribution; (c) aggregate contribution; and (d) fluorescence decay for image (○) a; (□) b; and (Δ) c.

maximum at 598±12 nm. The decay is multiexponential, and the mean lifetime is 1.77±0.8 ns. With MB, two bands are observed: at 608±16 and 739.5±1 nm. Again, the decay is multiexponential, lifetime 1.28±0.23 ns.

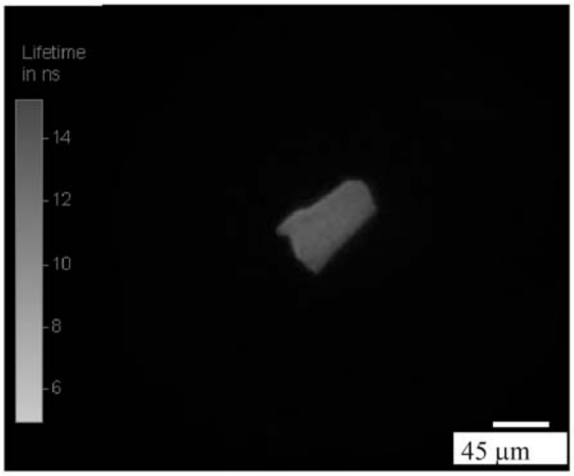

Fig. 10. Fluorescence of TMB crystal.

TMB microcrystals could also be obtained by evaporation of a concentrated dichloromethane solution. Figure 10 shows a fluorescing TMB crystal 50 μm in size.

The fluorescence intensity and lifetime are the same over the entire sample. The decay can be described as monoexponential, lifetime 9.5 ns. The fluorescence maximum is at 608±3 nm. Because of the strong absorption of the crystal, we failed to register the absorption spectrum, but the fluorescence spectrum of the spectrum of the crystal corresponds to the emission spectrum of the aggregate.

TMB with bulky substituents was prepared for fluorescence quenching due to π–π interactions. The emission spectrum of crystals of the resulting compound contained a single band. The fluorescence spectrum of this compound in solution is shifted red by 50 nm, implying aggregate formation. Unfortunately, we failed to obtain MB crystals, but MB films and crystal powder give two emission bands.

It is interesting to note that a crushed TMB microcrystal exhibits fluorescence. This fact provides strong evidence to show that the transfer from molecular crystal to powder gives rise to fluorescence quenching.

CONCLUSION

Novel sterically hindered BODIPY derivatives were prepared by the Trofimov reaction. This synthetic approach contributed to enhanced diversity of derivatives of the BODIPY family. One of such derivatives (MB), water-soluble and sensitive to Cu^{+2} ions in concentrations of about 1 nM, was used for the creation of a fluorescent nanosensor. Research into solid-phase optical properties of MB and TMB showed that such bulky substituents, as mesityl groups, in the pyrrole rings are big with consequences, by contrast alkyl substituents. Aromatic substituents favor formation of the crystal structure of TMB.

The behavior of TMB in the solid phase differs from that in solution, which differentiates this compound from MB. At the same time, the radiating ability is much decreased by defects in the solid phase. To approach this problem, we are presently developing new BODIPY derivatives having bulkier substituents. We tend to find a simple formula and develop an effective procedure for preparing fluorophore nanoensembles. The aim of our work is to obtain ultrasensitive nanosensors for determining *in vivo* such biologically important cations as intercellular calcium or such specific molecules as ATP.

REFERENCES

1. Valeur, B., *Molecular Fluorescence: Principles and Applications*, Weinheim: Wiley–VCH, 2001.
2. (a) Steinmeyer, R., Noskov, A., Krasel, C., Weber, I., Dees, C., and Harms, G.S., *J. Fluoresc.*, 2005, vol. 15, p. 707; (b) Houston, J.P., Ke, S., Wang, W., Li, C., and Sevick-Muraca, E.M., *J. Biomed. Opt.*, 2005, vol. 10, p. 054010.
3. *Applications of Fluorescence in the Biomedical Sciences*, Lansing Taylor, D., Waggoner, A.S., Lanni, F., Murphy, R.F., and Birge, R.R., Eds., New York: Liss, 1986.
4. *Applied Fluorescence in Chemistry, Biology and Medicine*, Rettig, W., Strehmel, B., Schrader, S., and Seifert, H., Eds., Berlin: Springer, 1999.
5. *Luminescence Applications in Biological, Chemical, Environmental, and Hydrological Sciences*, Goldberg, M.C., Ed., Washington, DC: American Chemical Society, 1989.
6. Slavík, J., *Fluorescence Microscopy and Fluorescent Probes*, New York: Plenum, 1999, vol. 2.
7. Newkome, G.R., Moorefield, C.R., and Vögtle, F., *Dendrimers and Dendrons*, Weinheim: Wiley–VCH, 2002.
8. (a) Sperling, L.H., *Introduction to Physical Polymer*

Science, New York: Wiley, 1992, 2nd ed.; (b) *Photophysics of Polymers*, Hoyle, C.E. and Torkelson, J.M., Eds., Washington, DC: American Chemical Society, 1987.

9. Pauchard, M., Huber, S., Méallet-Renault, R., Maas, H., Pansu, R.B., and Calzaferri, G., *Angew. Chem. Int. Ed.*, 2001, vol. 40, p. 2839.
10. *Optics of Semiconductors and Their Nanostructures*, Kalt, H. and Hetterich, M., Eds., Berlin: Springer, 2004, vol. 146.
11. *Substance colorée (d'origine minérale, organique ou métallique), généralement insoluble, qui colore la surface sur laquelle on l'applique, sans la pénétrer* (extrait de: Le Petit Robert dictionnaire de la langue française).
12. Laurent, G., Ha Duong, T., Méallet-Renault, R., and Pansu, R., *Nanophotonics: Integrating Photochemistry, Optics, and Nano/BioMaterials Studies*, Masuhara, H. and Kawata, S., Eds., Amsterdam: Elsevier, 2004, p. 89.
13. Shirai, K., Matsuoka, M., and Fukunishi, K., *Dyes Pigments*, 1999, vol. 42, p. 95.
14. Förster, T., *Fluoreszenz organischer Verbindung*, Göttingen: Vandenhoeck and Ruprecht, 1951, p. 166.
15. (a) Ullrich, G. and Ziessel, R., *J. Org. Chem.*, 2004, vol. 69, p. 2070; (b) Costela, A., Garcia-Moreno, I., Gomez, C., Sastre, R., Amat-Guerri, F., Liras, M., Arbeloa, F.L., Prieto, J.B., and Arbeloa, I.L., *J. Phys. Chem. A*, 2002, vol. 106, p. 7736.
16. Kollmansberger, M., Rurack, K., Resh-Genger, U., and Daub, J., *J. Phys. Chem. A,* 1998, vol. 102, p. 10211.
17. (a) Jakubiak, R., Bao, Z., and Rothberg, L., *Synth. Met.*, 2000, vol. 114, p. 61; (b) Langhals, H., Ismael, R., and Yuruk, O., *Tetrahedron*, 2000, vol. 56, p. 5435.
18. Méallet-Renault, R., Pansu, R.B., Amigoni-Gerbier, S., and Larpent, C., *Chem. Commun.*, 2004, vol. 20, p. 2344.
19. Chen, J., Burghart, A., Derecskei-Kovacs, A., and Burgess, K., *J. Org. Chem.*, 2000, vol. 65, p. 2900.
20. (a) Burghart, A., Kim, H., Welch, M.B., Thoresen, L.H., Reibenspies, J., Burgess, K., Bergstrom, F., and Johansson, L.B.-A., *J. Org. Chem.*, 1999, vol. 64, p. 7813; (b) Chen, J., Burghart, A., Derecskei-Kovacs, A., and Burgess, K., *J. Org. Chem.*, 2000, vol. 65, p. 2900.
21. Méallet-Renault, R., Hérault, A., Vachon, J.J., Pansu, R.B., Amigoni-Gerbier, S., and Larpent, C., *Photochem. Photobiol. Sci.*, 2006, vol. 5, p. 300.
22. (a) Trofimov, B.A., *Adv. Heterocycl. Chem.*, 1990, vol. 51, p. 177; (b) Trofimov, B.A., The *Chemistry of Heterocyclic Compounds*, Jones, R.A., Ed., Wiley: New York, 1992, part 2, vol. 48, p. 131.
23. Schmidt, E.Y., Zorina, N.V., Zaitsev, A.B., Mikhaleva, A.I., Vasil'tsov, A.M., Audebert, P., Clavier, G., Méallet-Renault, R., and Pansu, R.B., *Tetrahedron Lett.,* 2004, vol. 45, p. 5489.
24. Frisch, M.J., Trucks, G.W., Schlegel, H.B., Scuseria, G.E., Robb, M.A., Cheeseman, J.R., Montgomery, J.A., Jr., Vreven, T., Kudin, K.N., Burant, J.C., Millam, J.M., Iyengar, S.S., Tomasi, J., Barone, V., Mennucci, B., Cossi, M., Scalmani, G., Rega, N., Petersson, G.A., Nakatsuji, H., Hada, M., Ehara, M., Toyota, K., Fukuda, R., Hasegawa, J., Ishida, M., Nakajima, T., Honda, Y., Kitao, O., Nakai, H., Klene, M., Li, X., Knox, J.E., Hratchian, H.P., Cross, J.B., Adamo, C., Jaramillo, J., Gomperts, R., Stratmann, R.E., Yazyev, O., Austin, A.J., Cammi, R., Pomelli, C., Ochterski, J.W., Ayala, P.Y., Morokuma, K., Voth, G.A., Salvador, P., Dannenberg, J.J., Zakrzewski, V.G., Dapprich, S., Daniels, A.D., Strain, M.C., Farkas, O., Malick, D.K., Rabuck, A.D., Raghavachari, K., Foresman, J.B., Ortiz, J.V., Cui, Q., Baboul, A.G., Clifford, S., Cioslowski, J., Stefanov, B.B., Liu, G., Liashenko, A., Piskorz, P., Komaromi, I., Martin, R.L., Fox, D.J., Keith, T., Al-Laham, M.A., Peng, C.Y., Nanayakkara, A., Challacombe, M., Gill, P.M.W., Johnson, B., Chen, W., Wong, M.W., Gonzalez, C., and Pople, J., *Gaussian 03*, Rev. C.02, Wallingford, CT: Gaussian, 2004.
25. Kee, H.L., Kirmaier, C., Yu, L., Thamyongkit, P., Youngblood, W.J., Calder, M.E., Ramos, L., Noll, B.C., Bocian, D.F., Scheidt, W.R., Birge, R.R., Lindsey, J.S., and Holten, D., *J. Phys. Chem. B*, 2005, vol. 109, p. 20433.
26. Banuelos Prieto, J., Lopez Arbeloa, F., Martinez Martinez, V., and Lopez Arbeloa, I., *Chem. Phys.*, 2004, vol. 296, p. 13.
27. Kim, H., Burghart, A., Welch, M.B., Reibenspies, J., and Burgess, K., *Chem. Commun.*, 1999, p. 1889.
28. Kasha, M., *Radiat. Res.*, 1963, vol. 20, p. 55.